a

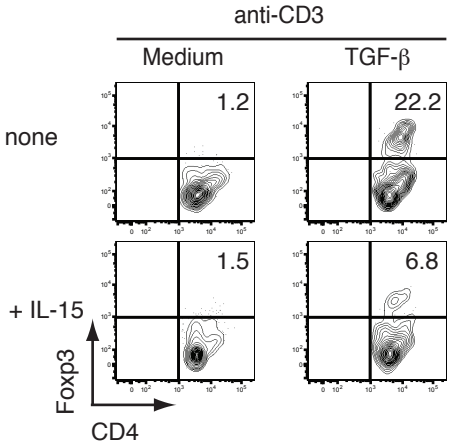
anti-CD3
Medium
TGF-β
none
1.2
22.2
+ IL-15
1.5
6.8
Foxp3
CD4

b

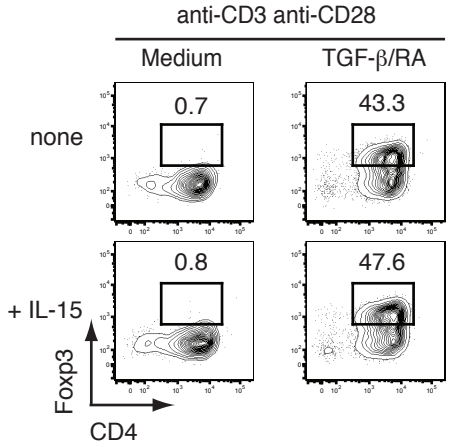
anti-CD3 anti-CD28
Medium
TGF-β/RA
none
0.7
43.3
+ IL-15
0.8
47.6
Foxp3
CD4

a

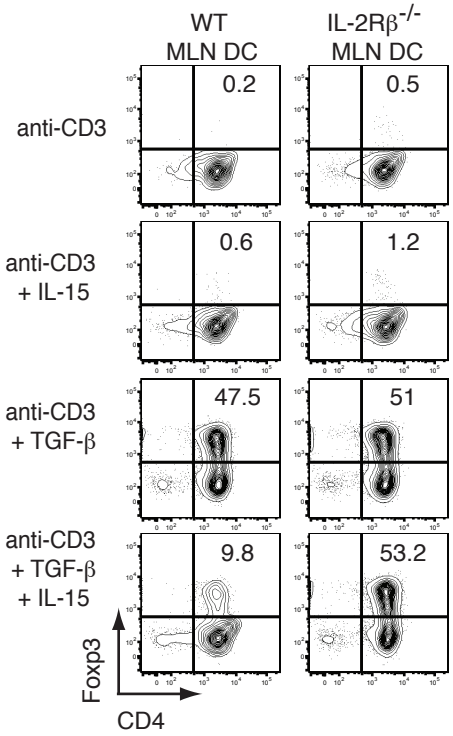
WT
MLN DC
IL-2Rβ-/-
MLN DC
anti-CD3
0.2
0.5
anti-CD3
+ IL-15
0.6
1.2
anti-CD3
+ TGF-β
47.5
51
anti-CD3
+ TGF-β
+ IL-15
9.8
53.2
Foxp3
CD4

b

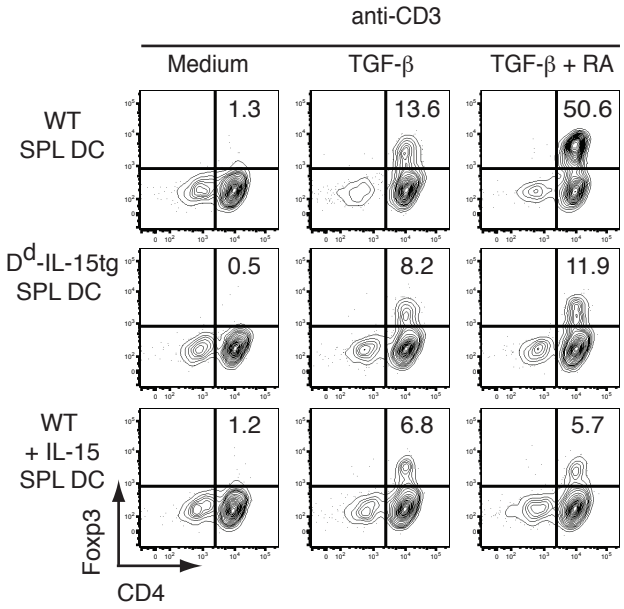
anti-CD3
Medium
TGF-β
TGF-β + RA
WT
SPL DC
1.3
13.6
50.6
Dd-IL-15tg
SPL DC
0.5
8.2
11.9
WT
+ IL-15
SPL DC
1.2
6.8
5.7
Foxp3
CD4

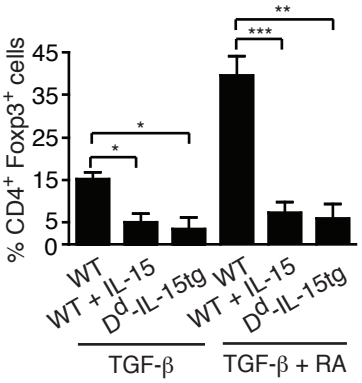
% CD4+ Foxp3+ cells
45
35
25
15
5
0
*
*
**
***
WT
WT + IL-15
Dd-IL-15tg
WT
WT + IL-15
Dd-IL-15tg
TGF-β
TGF-β + RA

c

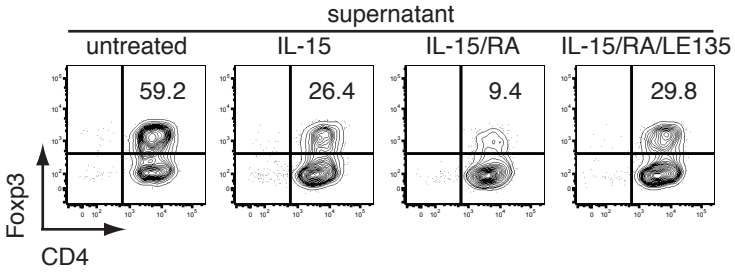
supernatant
untreated
IL-15
IL-15/RA
IL-15/RA/LE135
59.2
26.4
9.4
29.8
Foxp3
CD4

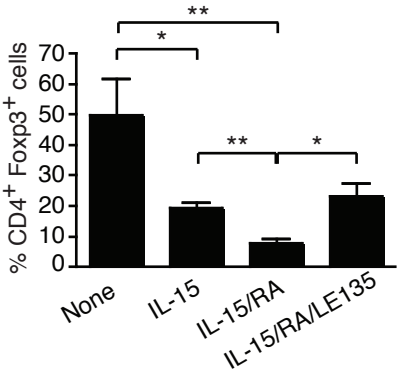
% CD4+ Foxp3+ cells
70
60
50
40
30
20
10
0
*
**
**
*
None
IL-15
IL-15/RA
IL-15/RA/LE135

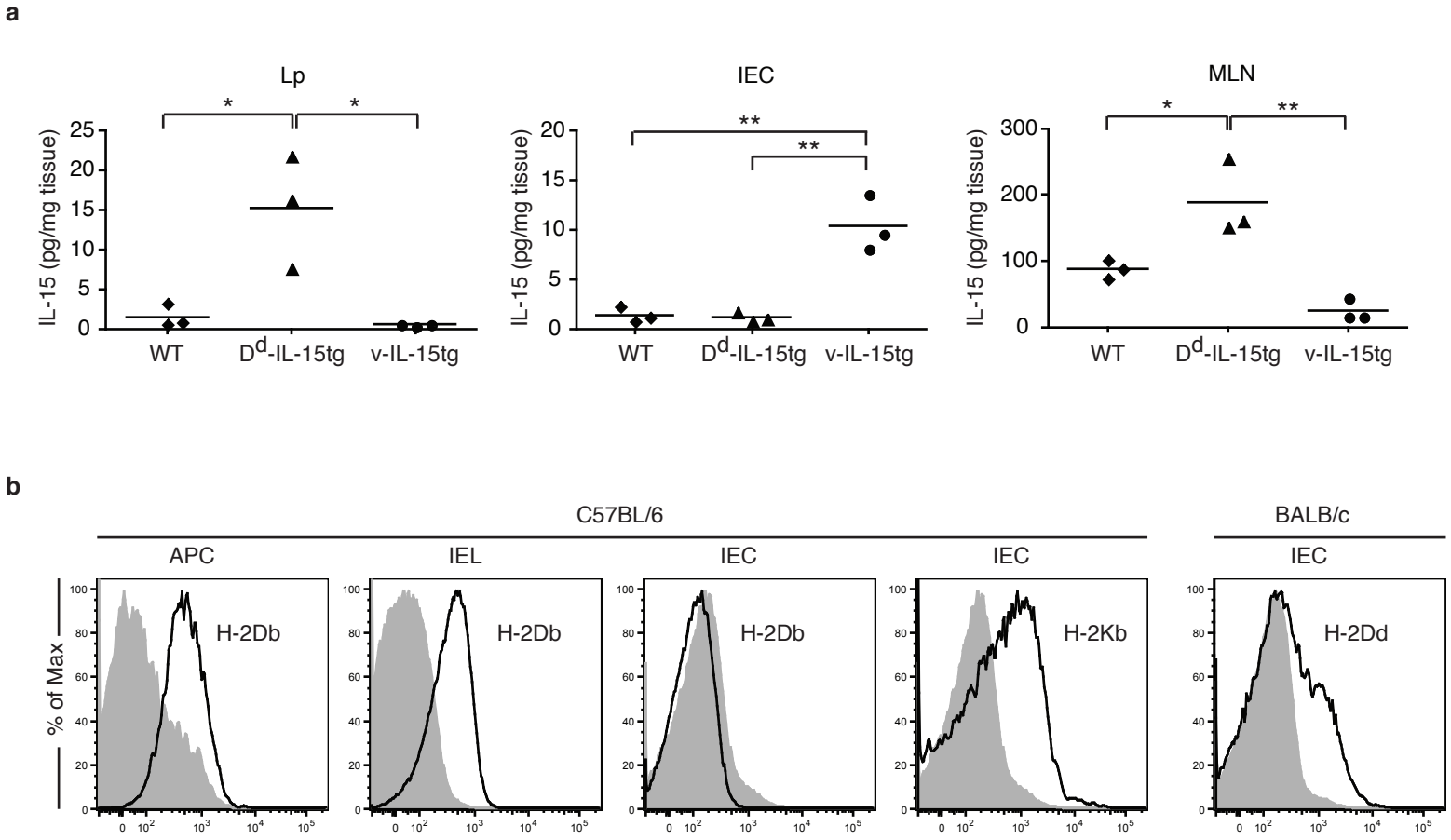
a
Lp
IEC
MLN
IL-15 (pg/mg tissue)
WT
Dd-IL-15tg
v-IL-15tg
b
C57BL/6
BALB/c
APC
IEL
IEC
IEC
IEC
% of Max
H-2Db
H-2Db
H-2Db
H-2Kb
H-2Dd

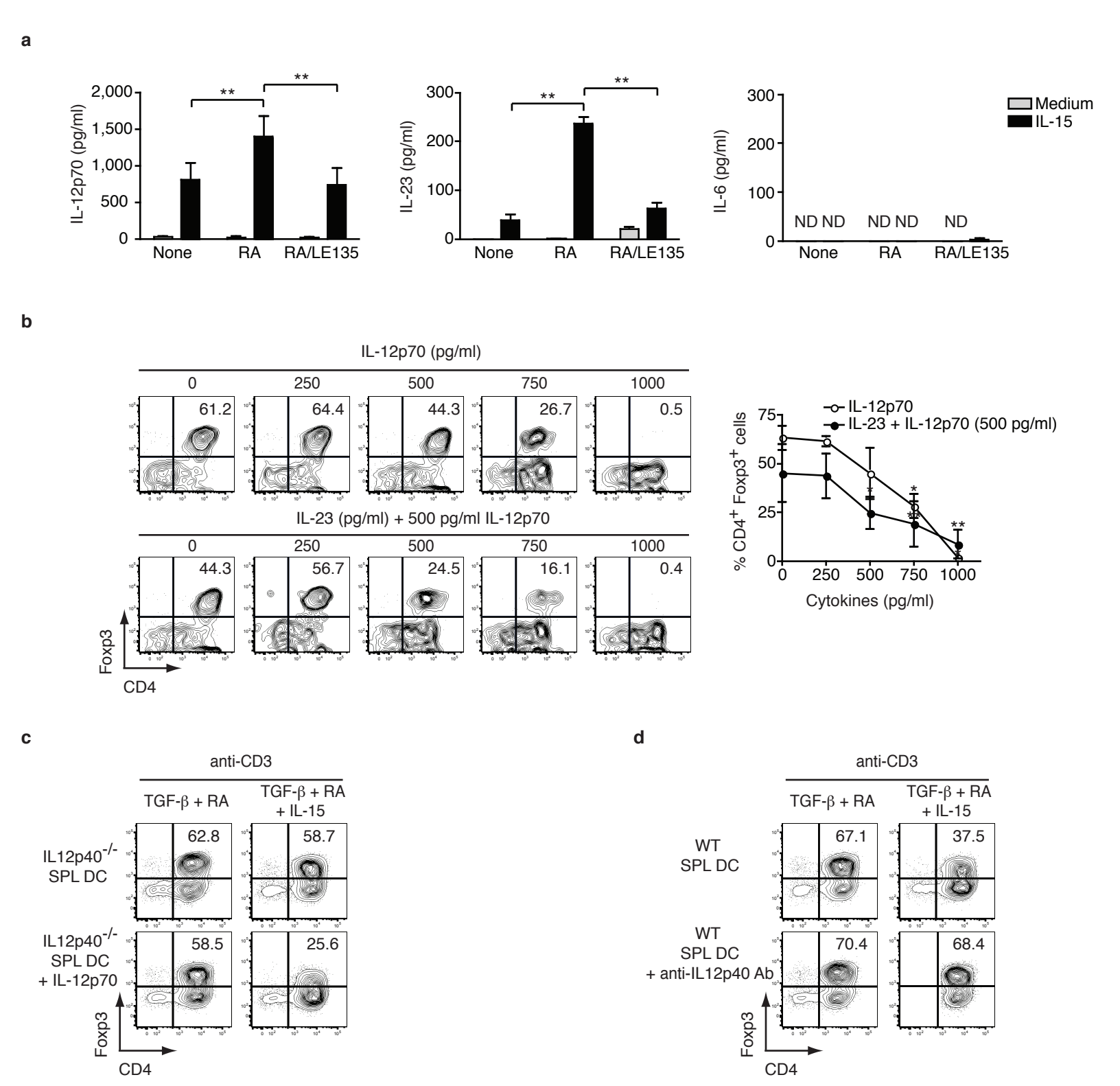

DePaolo et al., Supplementary Figure 4

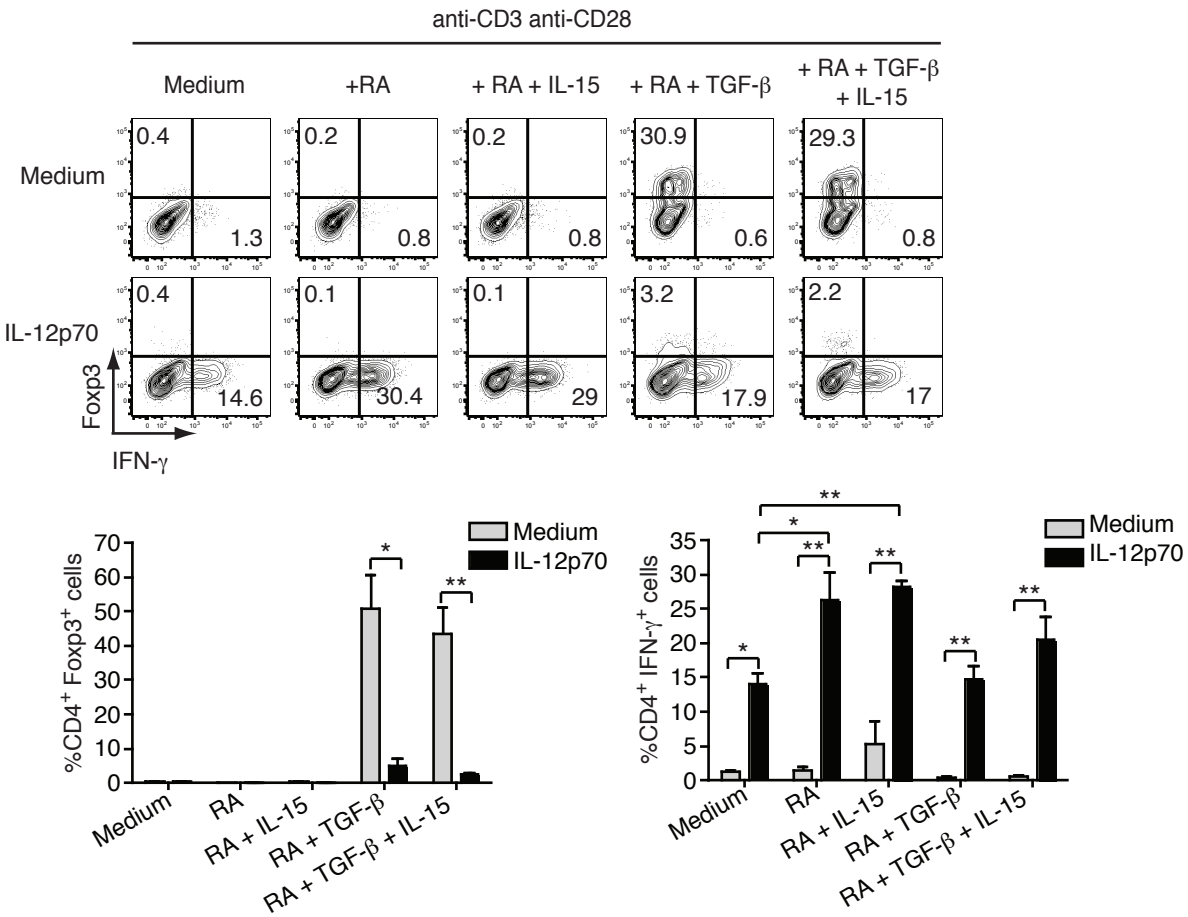
anti-CD3 anti-CD28
Medium
+RA
+ RA + IL-15
+ RA + TGF-β
+ RA + TGF-β + IL-15
Medium
IL-12p70
0.4
1.3
0.2
0.8
0.2
0.8
30.9
0.6
29.3
0.8
0.4
14.6
0.1
30.4
0.1
29
3.2
17.9
2.2
17
Foxp3
IFN-γ
%CD4+ Foxp3+ cells
%CD4+ IFN-γ+ cells
Medium
IL-12p70
Medium
RA
RA + IL-15
RA + TGF-β
RA + TGF-β + IL-15

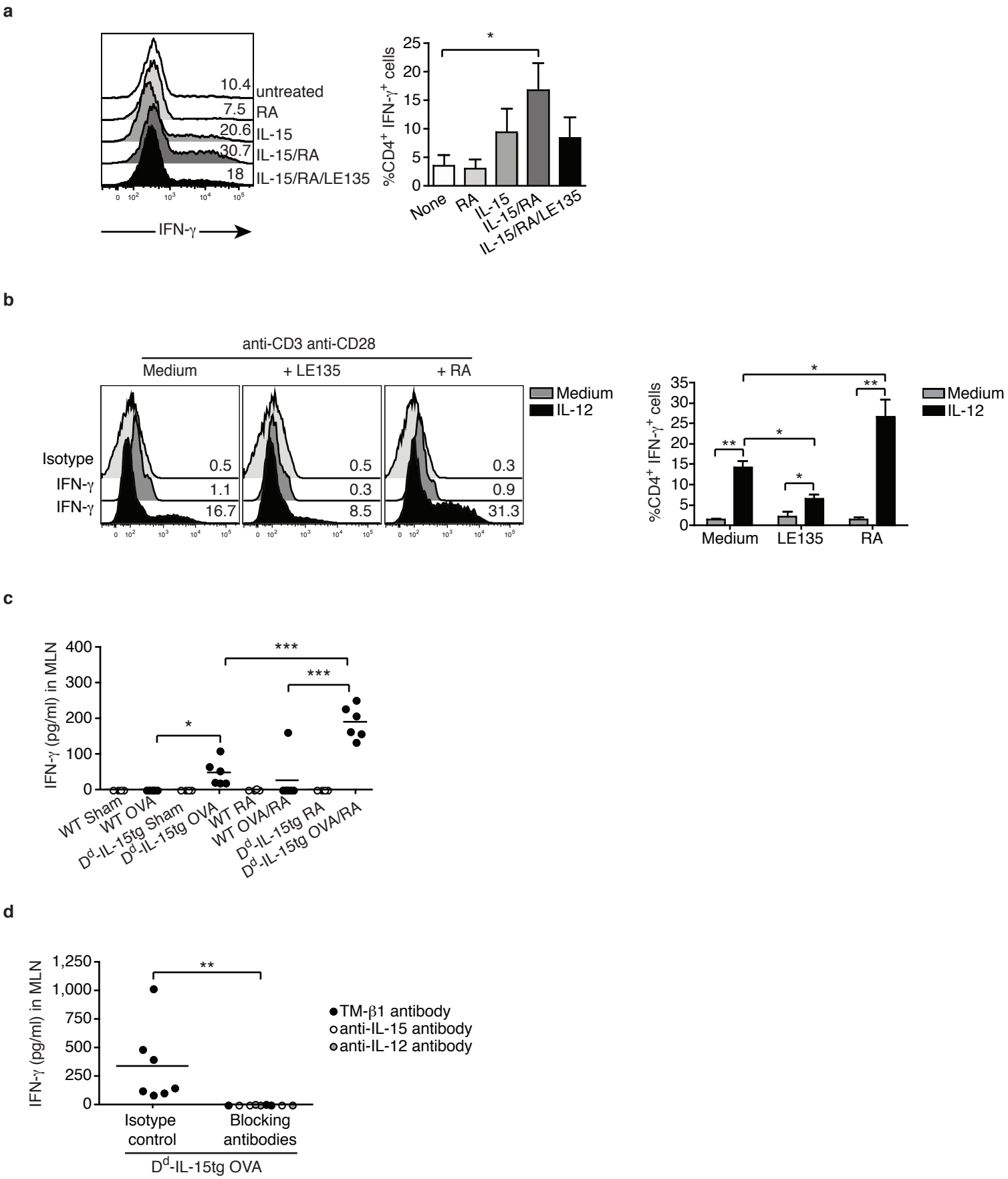
a
10.4
untreated
7.5
RA
20.6
IL-15
30.7
IL-15/RA
18
IL-15/RA/LE135
IFN-γ
%CD4+ IFN-γ+ cells
None
RA
IL-15
IL-15/RA
IL-15/RA/LE135
b
anti-CD3 anti-CD28
Medium
+ LE135
+ RA
Medium
IL-12
Isotype
IFN-γ
IFN-γ
0.5
0.5
0.3
1.1
0.3
0.9
16.7
8.5
31.3
%CD4+ IFN-γ+ cells
Medium
LE135
RA
c
IFN-γ (pg/ml) in MLN
WT Sham
WT OVA
Dd-IL-15tg Sham
Dd-IL-15tg OVA
WT RA
WT OVA/RA
Dd-IL-15tg RA
Dd-IL-15tg OVA/RA
d
IFN-γ (pg/ml) in MLN
TM-β1 antibody
anti-IL-15 antibody
anti-IL-12 antibody
Isotype control
Blocking antibodies
Dd-IL-15tg OVA

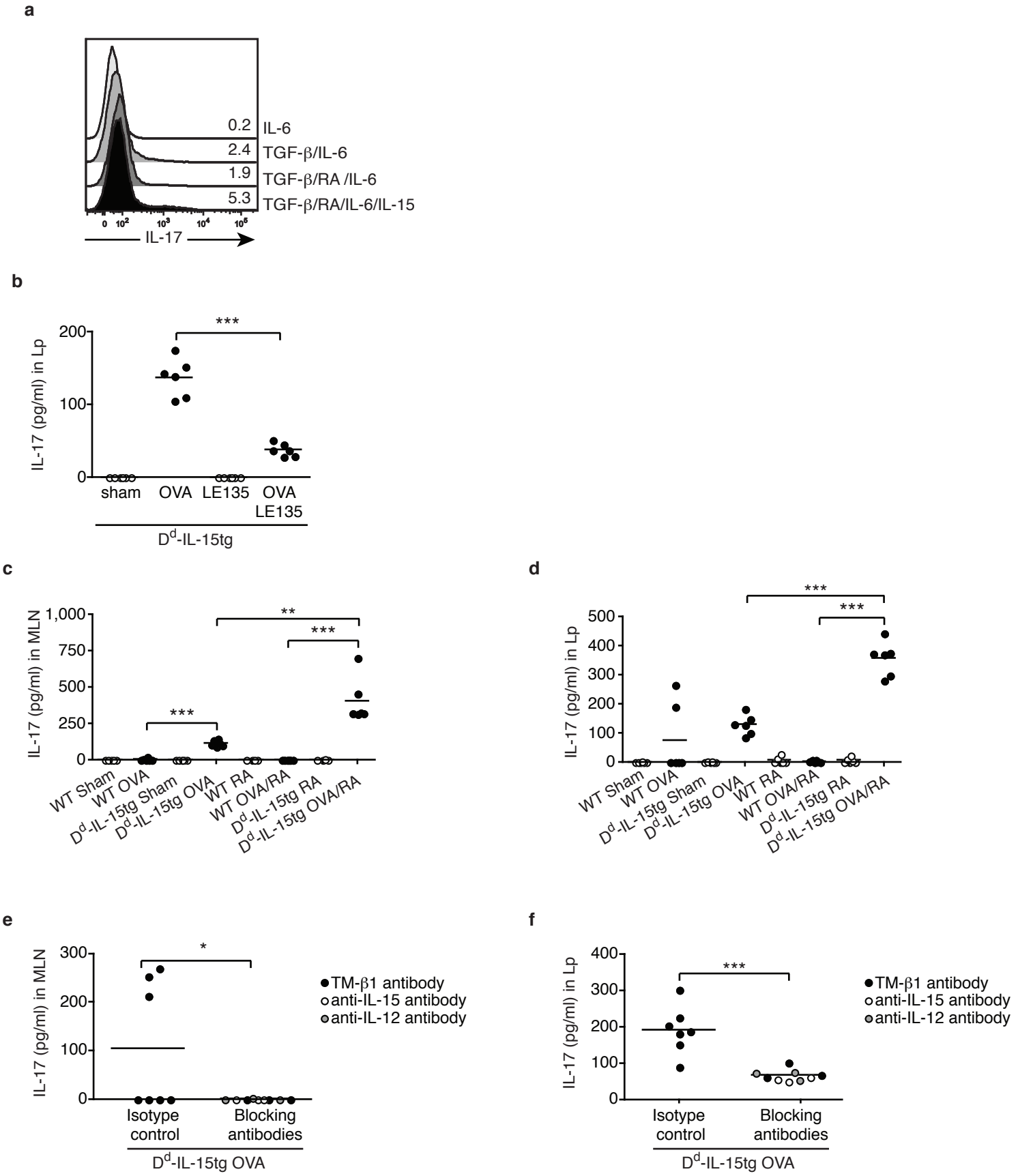
a
0.2
IL-6
2.4
TGF-β/IL-6
1.9
TGF-β/RA /IL-6
5.3
TGF-β/RA/IL-6/IL-15
0
10²
10³
10⁴
10⁵
IL-17
b
IL-17 (pg/ml) in Lp
200
100
0
***
sham
OVA
LE135
OVA LE135
D^d-IL-15tg
c
IL-17 (pg/ml) in MLN
1,000
750
500
250
0
**
***
***
WT Sham
WT OVA
D^d-IL-15tg Sham
D^d-IL-15tg OVA
WT RA
WT OVA/RA
D^d-IL-15tg RA
D^d-IL-15tg OVA/RA
d
IL-17 (pg/ml) in Lp
500
400
300
200
100
0
***
***
WT Sham
WT OVA
D^d-IL-15tg Sham
D^d-IL-15tg OVA
WT RA
WT OVA/RA
D^d-IL-15tg RA
D^d-IL-15tg OVA/RA
e
IL-17 (pg/ml) in MLN
300
200
100
0
*
Isotype control
Blocking antibodies
D^d-IL-15tg OVA
TM-β1 antibody
anti-IL-15 antibody
anti-IL-12 antibody
f
IL-17 (pg/ml) in Lp
400
300
200
100
0
***
Isotype control
Blocking antibodies
D^d-IL-15tg OVA
TM-β1 antibody
anti-IL-15 antibody
anti-IL-12 antibody

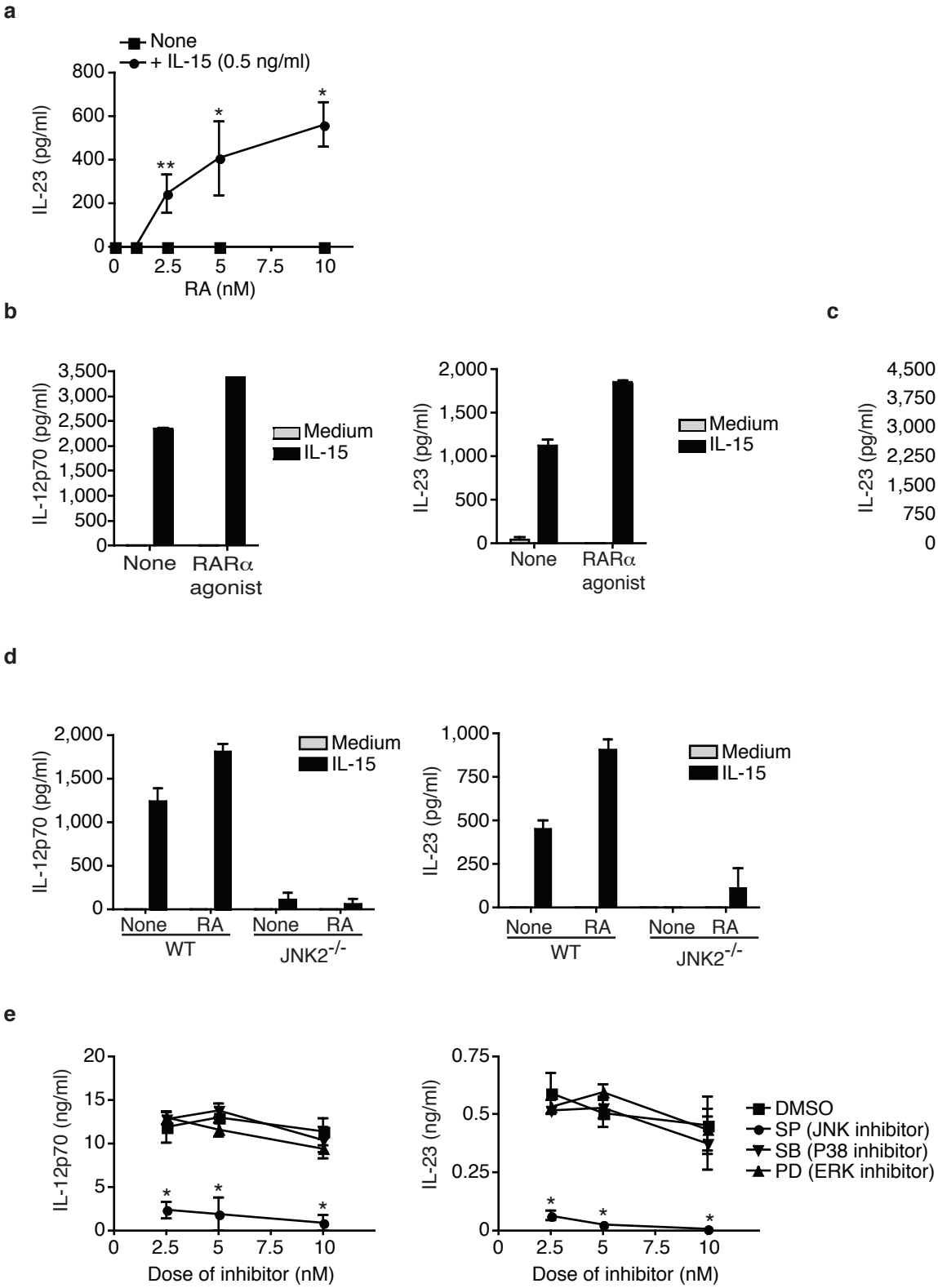
a
None
+ IL-15 (0.5 ng/ml)
IL-23 (pg/ml)
RA (nM)
b
IL-12p70 (pg/ml)
Medium
IL-15
None
RARα agonist
IL-23 (pg/ml)
c
IL-23 (pg/ml)
None
RA
WT
RARα-/-
d
IL-12p70 (pg/ml)
JNK2-/-
e
IL-12p70 (ng/ml)
IL-23 (ng/ml)
Dose of inhibitor (nM)
DMSO
SP (JNK inhibitor)
SB (P38 inhibitor)
PD (ERK inhibitor)

a

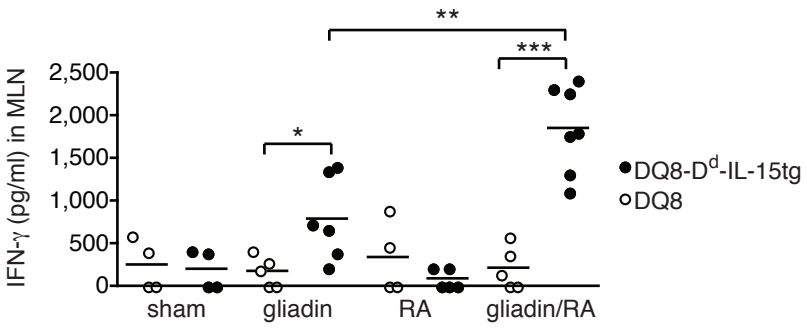

b

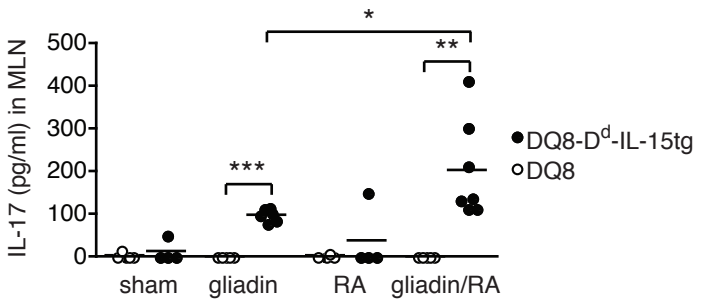

c

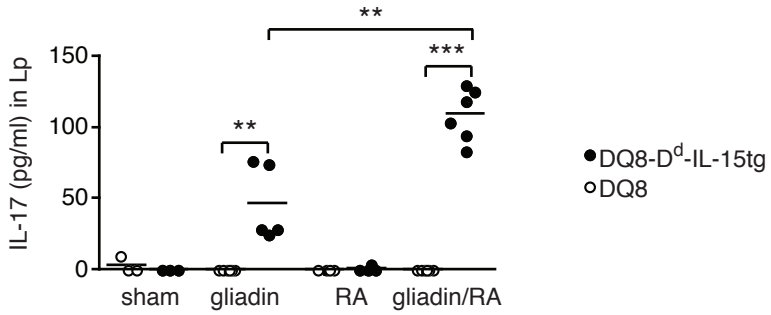

DePaolo et al., Supplemental Figure 9

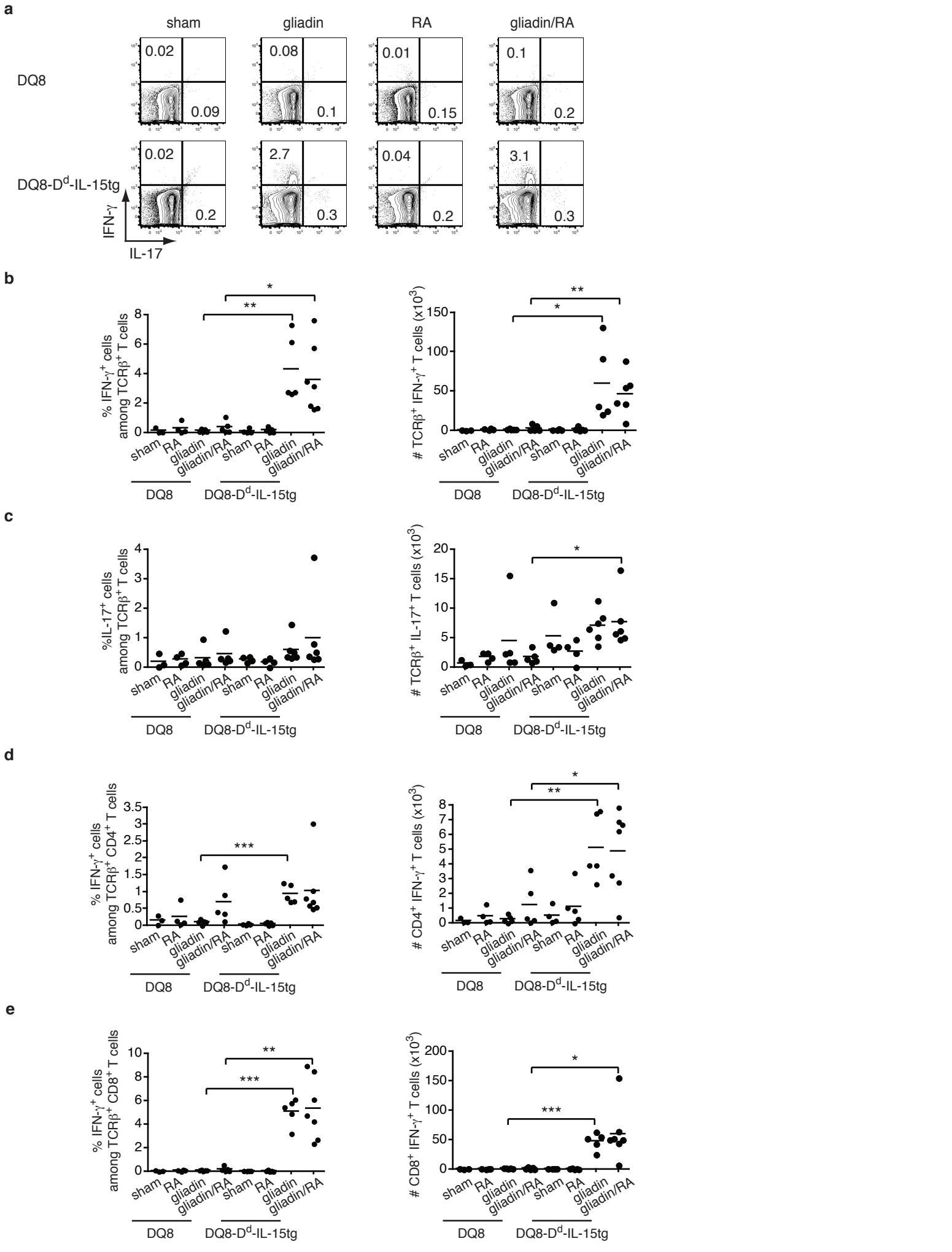

DePaolo et al., Supplementary Figure 10

a

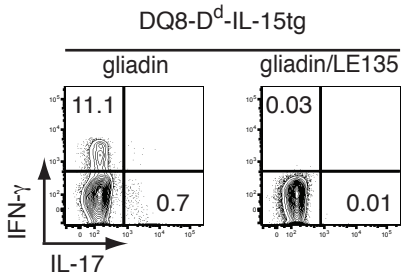
DQ8-D^d-IL-15tg
gliadin
gliadin/LE135
11.1
0.7
0.03
0.01
IFN-γ
IL-17

b

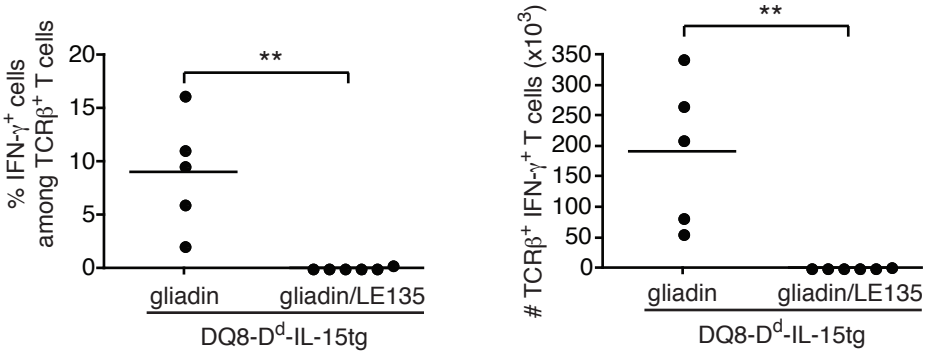
% IFN-γ$^+$ cells among TCRβ$^+$ T cells
**
gliadin
gliadin/LE135
DQ8-D^d-IL-15tg
TCRβ$^+$ IFN-γ$^+$ T cells (x10^3)
**
gliadin
gliadin/LE135
DQ8-D^d-IL-15tg

c

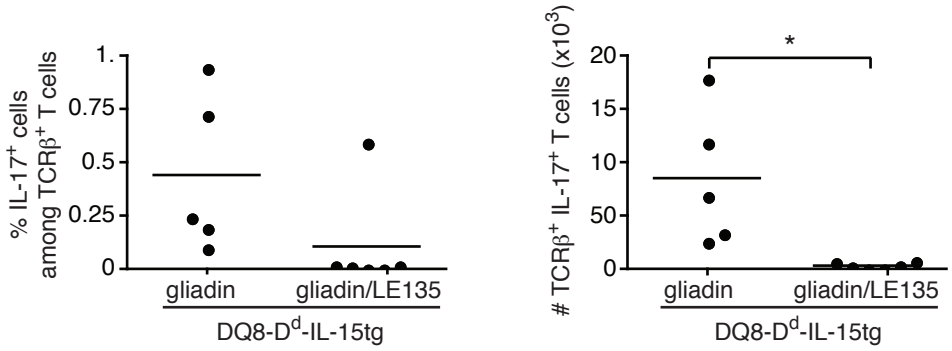
% IL-17$^+$ cells among TCRβ$^+$ T cells
gliadin
gliadin/LE135
DQ8-D^d-IL-15tg
TCRβ$^+$ IL-17$^+$ T cells (x10^3)
*
gliadin
gliadin/LE135
DQ8-D^d-IL-15tg

Supplementary figures:

Figure S1. IL-15-treated DC prevent conversion of naïve T cells into iTregs, whereas IL-15 does not affect iTreg generation in the absence of DC.

a, 10^5 $CD4^+$ $CD44^{lo}$ $Foxp3^-$ T cells were cultured with 4 x 10^4 MLN DC isolated from WT mice for three days with anti-CD3 alone or combined with IL-15 and TGF-β. The percentages of $Foxp3^+$ cells are indicated. One representative out of two independent experiments is shown. **b,** 2 x 10^5 $CD4^+$ $Foxp3^-$ T cells were cultured for three days with anti-CD3 and anti-CD28 alone or combined with TGF-β, RA, and IL-15. The percentages of $Foxp3^+$ cells are indicated. One representative out of three independent experiments is shown.

Figure S2. Evidence for the role of DC on iTreg conversion in the presence of IL-15

a, 10^5 $CD4^+$ $Foxp3^-$ T cells were cultured with 4 x 10^4 MLN DC isolated from WT or IL-2Rβ-deficient mice for three days with anti-CD3 alone or combined with IL-15 and TGF-β. The percentages of $Foxp3^+$ cells are indicated. One representative out of two independent experiments is shown. **b,** 10^5 $CD4^+$ $Foxp3^-$ T cells were cultured with 4 x 10^4 SPL DC isolated from WT or D^d-IL-15tg mice for three days with anti-CD3 alone or combined with IL-15, TGF-β and RA. The percentages of $Foxp3^+$ cells are shown. Graph depicts pooled data ± s.e.m. from three independent experiments. **c,** SPL DC isolated from WT mice were incubated overnight with IL-15 alone or combined with RA, or RA and a RA receptor antagonist, LE135. Supernatants were added to 2 x 10^5 $CD4^+$ $Foxp3^-$ T cells cultured for three days with anti-CD3, anti-CD28, TGF-β and RA. The percentages

of Foxp3$^+$ cells are indicated in each quadrant. Graph depicts pooled data ± s.e.m. from five independent experiments.

Figure S3. IL-15 expression in IL-15 transgenic mouse models

a, The expression of IL-15 in Lp, IEC, and MLN of WT, D^d-IL-15tg, and v-IL-15tg was assessed by ELISA. * P <0.05, ** P <0.01 (unpaired Student's t-test). **b,** The lack of IL-15 transgene expression in IEC of D^d-IL-15tg mice is due to the fact that the minimal ubiquitous MHC class I H-2D^d promoter used to drive IL-15 expression is inactive in IEC of C57BL/6 mice. The expression of MHC class I molecules (i.e. H2-D^d, H2-K^b, H2-D^d, open histograms) was assessed by flow cytometry on splenic APC (CD11c$^+$), intestinal IEL (CD45$^+$) and IEC (CD45$^-$ CD13$^+$) isolated from C57BL/6 mice and on IEC isolated from BALB/c mice. Filled histograms represent the corresponding isotype controls.

Figure S4. Effect of IL-15 and IL-12 on the generation of Foxp3$^+$ iTregs

a, SPL DC isolated from WT mice were incubated overnight with IL-15 alone or combined with RA or RA and RAR antagonist LE135. Levels of IL-12p70, IL-23, and IL-6 were measured by ELISA. Graph depicts data from at least three experiments performed independently ± s.e.m.. **b,** 2 x 10^5 CD4$^+$ Foxp3$^-$ T cells were cultured for 3 days with anti-CD3, anti-CD28, TGF-β, and RA, in the presence of increasing doses of IL-12p70, or 500 pg/ml IL-12p70 combined with increasing concentrations of IL-23. One representative out of three independent experiments is shown (left panel). Graph depicts pooled data ± s.e.m. from three independent experiments (right panel). **c,** 10^5 CD4$^+$ Foxp3$^-$ T cells were cultured with 4 x 10^4 SPL DC isolated from IL-12p40-deficient mice

for three days with anti-CD3 alone or combined with RA, TGF-β and IL-15 in the presence or absence of IL-12p70. The percentages of $Foxp3^+$ cells are indicated. One representative out of three independent experiments is shown. **d,** 10^5 $CD4^+$ $Foxp3^-$ T cells were cultured with 4 x 10^4 SPL DC isolated from WT mice for three days with anti-CD3 alone or combined with RA, TGF-β, and IL-15 in the presence or absence of anti-IL-12p40 antibody. The percentages of $Foxp3^+$ cells are indicated. One representative out of two independent experiments is shown.

Figure S5. Impact of IL-15 on T_H1 polarization

2 x 10^5 $CD4^+$ $Foxp3^-$ T cells were cultured for three days with anti-CD3 and anti-CD28 alone or combined with RA, IL-15, and TGF-β, in the presence of 500 pg/ml IL-12p70. The percentages of $Foxp3^+$ and IFN-γ^+ T cells are indicated. Bar graphs summarize the percentage of Foxp3-expressing $CD4^+$ T cells and the percentage of IFN-γ-producing $CD4^+$ T cells obtained from three independent experiments ± s.e.m.. * P <0.05, ** P <0.01, (unpaired Student's *t*-test).

Figure S6. Co-adjuvant effects of RA and IL-15 on T_H1 polarization.

a, WT SPL DC were incubated overnight with IL-15 alone or combined with RA, or RA and LE 135. Supernatants were added to 2 x 10^5 $CD4^+$ $Foxp3^-$ T cells cultured for three days with anti-CD3 and anti-CD28. The percentages of IFN-γ^+-producing $CD4^+$ T cells from three independent experiments ± s.e.m. is shown. **b,** 2 x 10^5 $CD4^+$ $Foxp3^-$ T cells were cultured for three days with anti-CD3 and anti-CD28 alone or combined with IL-15, RA and LE135 in the presence of 500 pg/ml IL-12p70. The percentages of $CD4^+$ IFN-γ^+

T cells are indicated. The graph summarizes the percentages of IFN-γ-producing $CD4^+$ T cells obtained from three independent experiments ± s.e.m.. **c,** WT and D^d-IL-15tg mice were fed OVA, RA, or a mixture of OVA and RA, five times during ten days. One day after the last feeding, MLN cells were harvested and re-stimulated for 48 h with OVA. Culture supernatants were assayed for IFN-γ by ELISA. The results are the means of triplicate samples obtained from two independent experiments. **d,** D^d-IL-15tg mice were fed OVA and received i.p. injections of anti-IL-12p40, anti-IL-15, or TMβ-1 (anti-IL-2Rβ) antibodies or isotype controls. As in (c), the levels of IFN-γ in the MLN were assessed by ELISA. When anti-IL-15 and anti-IL-12 treatment experiments were performed in parallel, control mice received a mixture of corresponding isotype controls. Data on individual mice from two independent experiments are shown, except for anti-IL-12 treatment that was performed on three individual mice.

* P <0.05, ** P <0.01, *** P <0.001 (unpaired Student's t-test).

Figure S7. Impact of IL-15 on T_H17 responses

a, $1x10^6$ purified $CD4^+$ T cells were stimulated with anti-CD3, anti-CD28, and IL-6, in the presence or absence of TGF-β, RA and IL-15. One representative out of two independent experiments is shown. **b,** D^d-IL-15tg mice were fed PBS (sham), OVA, LE135, or a mixture of OVA and LE135. The concentration of IL-17 in Lp culture supernatants was detected by ELISA. The results are the means of triplicate samples obtained from two independent experiments. **c-d,** D^d-IL-15tg and WT mice were fed PBS (sham), RA, OVA, or a mixture of OVA and RA five times during ten days. One day after the last feeding, MLN **(c)** and Lp **(d)** cells were harvested and re-stimulated with

OVA for 48 h and 24 h, respectively. Culture supernatants were assayed for IL-17 by ELISA. The results are the means of triplicate samples obtained from two independent experiments. **e-f,** D^d-IL-15tg mice were fed OVA and were treated i.p. with anti-IL-12p40, anti-IL-15, or TMβ-1 (anti-IL-2Rβ) antibodies. One day after the last feeding, MLN **(e)** and Lp **(f)** cells were harvested and re-stimulated with OVA for 48 h and 24 h, respectively. The concentration of IL-17 in the culture supernatants was detected by ELISA. When anti-IL-15 and anti-IL-12 treatment experiments were performed in parallel, control mice received a mixture of corresponding isotype controls. Data on individual mice from two independent experiments are shown, except for anti-IL-12 treatment that was performed on three individual mice.

*P<0.05, ** P <0.01, *** P <0.001 (unpaired Student's t-test).

Figure S8. The synergistic activation of JNK in DC by RA and IL-15 promotes inflammatory responses.

a, 10^5 SPL DC were incubated overnight with increasing doses of RA ranging from 1 to 10 nM RA alone, or combined with 0.5 ng/ml IL-15. The production of IL-23 in the culture supernatants was determined by ELISA. Results are mean values ± s.e.m. of three independent experiments. **b,** BMDC isolated from WT mice were stimulated overnight with IL-15 alone or with IL-15 and a RAR-α agonist (AM580). The production of IL-12p70 and IL-23 in the supernatants was measured by ELISA. Results are mean values ± s.e.m. of two independent experiments. **c,** BMDC isolated from WT and RARα-deficient mice were incubated overnight with IL-15 alone or IL-15 combined with RA. The levels

of IL-23 were measured in the culture supernatants by ELISA. Data are representative of two independent experiments ± s.e.m..

d, SPL DC isolated from JNK2-deficient mice were incubated overnight with IL-15 alone or in the presence of RA. IL-12p70 and IL-23 were measured in the culture supernatants by ELISA. Data are representative of three independent experiments ± s.e.m.. **e,** BMDC were pre-treated for 30 min with PD98059 (MEK1/2 inhibitor), SP600125 (JNK inhibitor), SB203580 (P38 inhibitor), or DMSO control and then incubated with IL-15. IL-12p70 and IL-23 production was determined 18 h later by ELISA. The values are means ± s.e.m. from three independent experiments.

*p<0.05, **p<0.01 (unpaired Student's *t*-test).

Figure S9. Inflammatory T cells are induced in DQ8-D^{d}-IL-15tg mice fed gliadin

DQ8 and DQ8-D^{d}-IL-15tg mice were fed PBS (sham), RA, gliadin, or a mixture of gliadin and RA. The MLN **(a-b)** and Lp **(c)** cells were harvested and re-stimulated with gliadin for 48 h or 24 h, respectively. Supernatants were analyzed for IFN-γ **(a)** and IL-17 **(b-c)** by ELISA. Data are representative of two experiments performed independently. *P<0.05, ** P <0.01, *** P <0.001 (unpaired Student's *t*-test)

Figure S10. Both CD4^{+} and CD8^{+} T cells producing IFN-γ are induced in DQ8-D^{d}-IL-15tg mice fed gliadin

DQ8 and DQ8-D^{d}-IL-15tg mice were fed PBS (sham), RA, gliadin, or a mixture of gliadin and RA. **a,** TCRβ^{+} T cells isolated from the MLN were analyzed by flow cytometry for IFN-γ and IL-17 expression. **b,** The percentages and absolute numbers of

IFN-γ-producing TCRβ$^+$ T cells in the MLN were determined by flow cytometry. Data are representative of two experiments performed independently. **c,** Percentages and absolute numbers of IL-17-producing TCRβ$^+$ T cells in the MLN of sham, RA, gliadin, and gliadin/RA fed mice. Data are representative of two experiments performed independently. **d,** The percentages and absolute numbers of IFN-γ-producing CD4$^+$ (upper panels) T cells in the MLN of fed mice were determined by flow cytometry. Data are representative of two experiments performed independently. **e,** The percentages and absolute numbers of IFN-γ-producing CD8$^+$ T cells in the MLN of fed mice were determined by flow cytometry. Data are representative of two experiments performed independently. *P<0.05, ** P <0.01, *** P <0.001 (unpaired Student's t-test).

Figure S11. IL-15 and RA synergize to induce IFN-γ-producing T cells in DQ8-D^d-IL-15tg mice fed gliadin

a, TCRβ$^+$ T cells isolated from the MLN of DQ8-D^d-IL-15tg mice fed gliadin or a combination of gliadin and LE135 were analyzed by flow cytometry for IFN-γ and IL-17 expression. The percentages and absolute numbers of TCRβ$^+$ T cells producing IFN-γ **(b)** and IL-17 **(c)** were determined by flow cytometry. Data are representative of two experiments performed independently. *P<0.05, **P<0.01, (unpaired Student's t-test)